UNIVERSAL WISER
PUBLISHER

Research Article

# Unveiling Eco-Friendly Energy Storage Using (Ge/Sn/Pb)-Doped SiC Nanocomposites Through Hydrogen Adsorption: Materials Modeling by DFT Study

**Fatemeh Mollaamin**[ID]

Department of Biomedical Engineering, Faculty of Engineering and Architecture, Kastamonu University, Kastamonu, Turkey
E-mail: fmollaamin@kastamonu.edu.tr

**Abstract:** As applied materials for quantum nanotechnology, silicon carbide nanocage (Si-C_NC), germanium carbide nanocage (Ge-C_NC), tin carbide nanocage (Sn-C_NC) or lead carbide nanocage (Pb-C_NC) have attracted considerable attention in materials science. A comprehensive investigation on hydrogen grabbing by main group carbides of Si, Ge, Sn or Pb was carried out including using density functional theory (DFT) computations at the Coulomb-Attenuating method with the hybrid functional Becke 3-parameter Lee-Yang-Parr, Electron Paramagnetic Resonance (CAM-B3LYP)/EPR-III), 6-311+G (d, p), and Los Alamos National Laboratory 2 double $\zeta$ (LANL2DZ) level of theory. The data represents that if silicon elements are replaced by germanium, tin or lead, the H-grabbing energy will be ameliorated. Electromagnetic and thermodynamic properties of Si-C_NC, Ge-C_NC, Sn-C_NC, Pb-C_NC and H@Si-C_NC, H@Ge-C_NC, H@Sn-C_NC, H@Pb-C_NC clusters were analyzed. The hypothesis of the adsorption phenomenon was confirmed by density distributions of the density of states (DOS) and partial density of states (PDOS) and charge distribution. The fluctuation in charge density values demonstrates that the electronic densities were mainly located in the boundary of adsorbate/adsorbent atoms during the adsorption status. All in all, the consequences display that the Si-C_NC, Ge-C_NC, Sn-C_NC or Pb-C_NC might be appropriate candidate nanocones for hydrogen storage. This study proves that the application of silicon carbide, germanium carbide, tin carbide or lead carbide nanocages in supercapacitor devices has great potential in the field of energy storage, providing a reference for the further development of novel semiconductors in the field of energy storage and optoelectronic devices.

*Keywords*: hydrogen storage, DFT computation, carbide nanocage

## 1. Introduction

Designing advanced electrode materials that can be reliably cycled at high temperatures and used for assembling advanced energy storage devices remains a major challenge. As a representative of novel wide bandgap semiconductors, silicon carbide, germanium carbide, tin carbide or lead carbide nanocages have broad prospects in energy storage due to their excellent characteristics of stable chemical properties.

A type of clean fuel is hydrogen that might be employed to accumulate, carry, and spread energy produced by other sources and it generates water when applied in a fuel cell.[1] A fuel cell applies reverse electrolysis to convert an oxidizing agent and hydrogen to power an electric motor.[2-4]

CNTs owing to their lightness, tube construction, vast plane and high reactivity between C and H atoms can be proposed as an estimated material for H-grabbing.[5-8] Biofuel cells have been in the spotlight for the past century because of their potential and promise as a unique platform for sustainable energy harvesting from the human body and the environment. Because biofuel cells are typically developed in a small platform serving as a primary battery with limited fuel or as a rechargeable battery with repeated refueling, they have been interchangeably named biobatteries.[9-12]

It was investigated that H-storing on the C-nano compound indicates molecular hydrogen dissociation.[13-16] The structure of transition metal-carbon exhibits a charge distribution among boundary atoms and the cationic state of transition metals can be discussed.[17-21] Thus, the electronic charge can be produced through gas molecules adsorption on the surfaces of ionic transition metal.[22-24] Transition metals as dopants might make a whole Hamiltonian perturbation towards alterations in electronic structures, which convert it a substantial usage in magnetic electronic instruments.[25-29] Recently, Si-, Ge- or Sn-carbide nanostructures have been suggested as engaged H-grabbing compounds.[30-32] Since the polarizability of silicon is more than carbon, it is supposed that Si-C/Si nanosheet might attach to compositions more strongly in comparison to the net carbon nano-surfaces.[33-35]

Therefore, during this work we are going to apply computational methods towards estimating the efficiency of Si-C_NC, Ge-C_NC, Sn-C_NC and Pb-C_NC clusters for H-grabbing. The calculation has measured the magnetic and electronic structures of H@Si-C_NC, H@Ge-C_NC, H@Sn-C_NC and H@Pb-C_NC clusters by DFT study,[36] generalized gradient approximation (GGA) potential and Perdew-Burke-Ernzerhof (PBE) functional.[37,38] Moreover, it must be remarked that metal hydrides are still in their early steps of development, and further investigation is needed to evaluate their commercial viability.[39-44]

This work wants to construct Si-C_NC, Ge-C_NC, Sn-C_NC or Pb-C_NC complexes through hydrogen adsorption calculations. The article intends to illustrate the technical part of computation, and investigate the Si-C_NC, Ge-C_NC, Sn-C_NC or Pb-C_NC complexes. Then, hydrogen storage is reported through hydrogen adsorption calculations and employing molecular electrostatic potential energy and molecular orbitals computations.

## 2. Theoretical conception, materials, and methods

In Figure 1, nano-carbides of silicon, germanium, tin or lead have been designed by disclination angle of $180^\circ$, cone height of 20 Å and MWNC (1, 5).

The H-grabbing on the surface of Si-C_NC, Ge-C_NC, Sn-C_NC, Pb-C_NC indicated the chemisorption between H-atoms and Si-C_NC, Ge-C_NC, Sn-C_NC, Pb-C_NC using the GaussView 6.06.16[45] and Gaussian 16, Revision C.01[46] and DFT computations at the CAM-B3LYP/EPR-III, 6-311+G (d, p), LANL2DZ level of theory.[47,48]

The charge transfer between H-atoms and Si-C_NC, Ge-C_NC, Sn-C_NC or Pb-C_NC is computed by Bader charge parameter.[49-51] The alterations of charge density have demonstrated that Si-C_NC shows the Bader charge of -0.667 coulomb, before H-adsorption, and -0.674 coulomb after H-adsorption, respectively. Ge-C represents the Bader charge of -0.631 coulomb before H-adsorption, and -0.652 coulomb after H-adsorption, respectively. Sn-C indicates the Bader charge of -0.829 coulomb before H-adsorption, and -0.858 coulomb after H-adsorption, respectively. Pb-C has the Bader charge of -0.913 coulomb before H-adsorption, and -0.923 coulomb after H-adsorption, respectively. Thus, the alterations of charge density for H-grabbing on Si-C_NC, Ge-C_NC, Sn-C_NC or Pb-C_NC are $\Delta Q_{H@Si-C\_NC}$ = -0.007e > $\Delta Q_{H@Sn-C\_NC}$ = -0.029e > $\Delta Q_{H@Ge-C\_NC}$ = -0.021e > $\Delta Q_{H@Pb-C\_NC}$ = -0.01e. Si-C_NC, Ge-C_NC, Sn-C_NC or Pb-C_NC have played the role of electron acceptors while H-atoms as the stronger electron donors have appeared through adsorption on these nano-carbides. In fact, diffusion of the H atoms from the most stable adsorption site to the nearest neighbouring site was studied in order to obtain diffusion barrier and diffusion values.
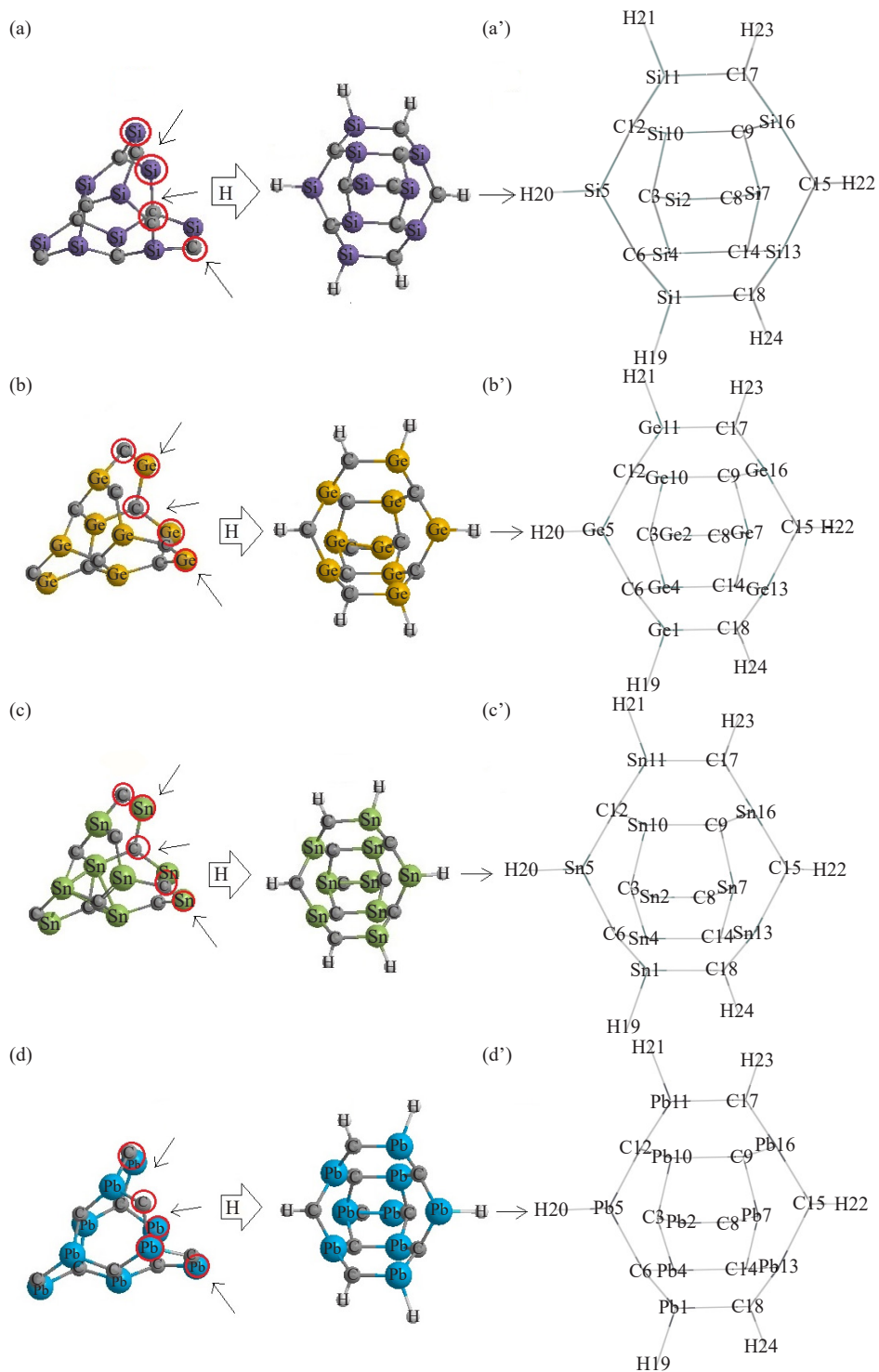
**Figure 1.** H-grabbing by (a) Si-C_NC, (b) Ge-C_NC, (c) Sn-C_NC, (d) Pb-C_NC towards formation of (a') H@Si-C_NC, (b') H@Ge-C_NC, (c') H@Sn-C_NC, and (d') H@Pb-C_NC

# 3. Results and discussions

## 3.1 *Electronic characterization of nano-carbides*

It is clear from Figure 2 that after H-grabbing by Si-C_NC, Ge-C_NC, Sn-C_NC or Pb-C_NC, there is a significant
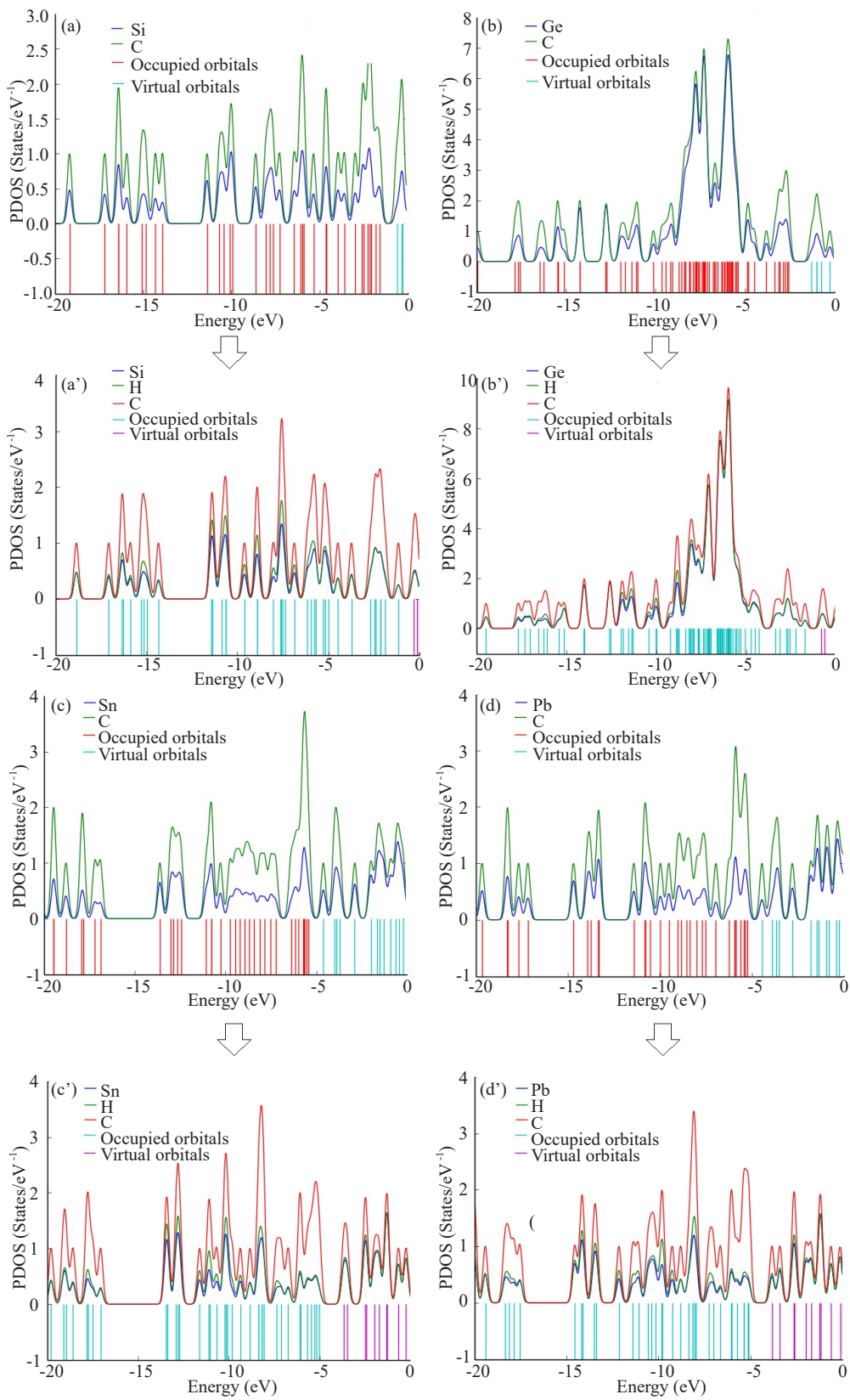
**Figure 2.** PDOS adsorption of (a) Si-C_NC, (a') H@Si-C_NC, (b) Ge-C_NC, (b') H@Ge-C_NC, (c) Sn-C_NC, (c') H@Sn-C_NC, (d) Pb-C_NC and (d') H@Pb-C_NC complexes

contribution of Ge, Sn, Pb d-orbital in the unoccupied level. Density of states (DOS) resulted that Si, Ge, Sn, Pb stay in the ionic form towards admitting more electrons from other particles (Figure 2a-d, a'-d').

Figure 2(a) and (a') shows that the Si-C_NC and H@Si-C_NC states, respectively, have more contribution at the conduction band around -5 to -15 eV, while contribution of C-states is wide, and Si- and H-states possess less contributions. The nanostructures of Ge-C_NC (Figure 2b), H@Ge-C_NC (Figure 2b'), Sn-C_NC (Figure 2c), H@Sn-C_NC (Figure 2c'), Pb-C_NC (Figure 2d) and H@Pb-C_NC (Figure 2d'), respectively, possess high contribution at the middle of the conduction band between -5 to -10 eV, while contribution of carbon sates are wide with high distribution around -7 eV, and Ge-, Sn- or Pb-states have less contributions in comparison to C-states. The projected density of states shows that the H atoms with 1s orbital electrons will hybridize with C/Si/Ge/Sn/Pb atoms with the 2p/3p/3d/4d/5d for orbital electrons of the nearby surface. The climbing image nudged elastic band study shows that the surface free H atoms are very easy to diffuse between the surface short-bridge sites and the subsurface short-bridge sites but the diffusion between the short-bridge site and the triangular center site is extremely difficult.

## 3.2 NQR analysis

NQR parameters of gas molecules of H-grabbing on Si-C_NC, Ge-C_NC, Sn-C_NC, Pb-C_NC based on cartesian harmonies are:[52]

$$V(r) = V(0) + \left[ \left( \frac{\partial V}{\partial x_i} \right)\Big|_0 \cdot x_i \right] + \frac{1}{2} \left[ \left( \frac{\partial^2 V}{\partial x_i x_j} \right)\Big|_0 \cdot x_i x_j \right] + \dots \tag{1}$$

$$U = -\frac{1}{2} \int_{\mathcal{D}} d^3 r \rho_r \left[ \left( \frac{\partial^2 V}{\partial x_i^2} \right)\Big|_0 \cdot x_i^2 \right] = -\frac{1}{2} \int_{\mathcal{D}} d^3 r \rho_r \left[ \left( \frac{\partial E_i}{\partial x_i} \right)\Big|_0 \cdot x_i^2 \right] = -\frac{1}{2} \left( \frac{\partial E_i}{\partial x_i} \right)\Big|_0 \cdot \int_{\mathcal{D}} d^3 r \left[ \rho(r) \cdot x_i^2 \right] \tag{2}$$

$$\chi = e^2 Q q_{zz} / h \tag{3}$$

$$\eta = q_{xx} - q_{yy} / q_{zz} \tag{4}$$

where $\chi$, quadrupole coupling constant; $\eta$, asymmetry factor of the electric field gradient tensor; $q_{ii}$, ingredients of the electric field gradient tensor; $e$, the proton charge; $h$, the Planck's constant and $Q$, the nuclear quadrupole moment are the NQR parameters.[52]

**Table 1.** The parameters of electric potential ($E_p$) and Bader charge ($Q$) of H-grabbing on the Si-C_NC, Ge-C_NC, Sn-C_NC, Pb-C_NC using "CAM-B3LYP/EPR-III, 6-311+G (d, p), LANL2DZ" computations

| Si-C_NC | | | H@Si-C_NC | | | Ge-C_NC | | | H@Ge-C_NC | | |
|---|---|---|---|---|---|---|---|---|---|---|---|
| Atom | $Q$ | $E_p$ | Atom | $Q$ | $E_p$ | Atom | $Q$ | $E_p$ | Atom | $Q$ | $E_p$ |
| Si(1) | 0.3110 | −48.583 | Si(1) | 0.4335 | −48.5485 | Ge(1) | 0.2338 | −153.986 | Ge(1) | 0.3472 | −153.99 |
| Si(2) | 0.5853 | −48.6074 | Si(2) | 0.5886 | −48.6244 | Ge(2) | 0.4877 | −153.629 | Ge(2) | 0.4919 | −153.637 |
| C(3) | −0.4429 | −14.6956 | C(3) | −0.4439 | −14.6901 | C(3) | −0.3721 | −14.634 | C(3) | −0.3724 | −14.6381 |
| Si(4) | 0.4601 | −48.4976 | Si(4) | 0.4694 | −48.5212 | Ge(4) | 0.4184 | −153.917 | Ge(4) | 0.3929 | −153.941 |

**Table 1.** (cont.)

| Si-C_NC | | | H@Si-C_NC | | | Ge-C_NC | | | H@Ge-C_NC | | |
|---|---|---|---|---|---|---|---|---|---|---|---|
| Atom | $Q$ | $E_p$ | Atom | $Q$ | $E_p$ | Atom | $Q$ | $E_p$ | Atom | $Q$ | $E_p$ |
| Si(5) | 0.3550 | −48.5651 | Si(5) | 0.4596 | −48.5393 | Ge(5) | 0.3336 | −154.015 | Ge(5) | 0.3576 | −153.98 |
| C(6) | −0.4512 | −14.7206 | C(6) | −0.4765 | −14.7486 | C(6) | −0.4001 | −14.6755 | C(6) | −0.4081 | −14.7029 |
| Si(7) | 0.6123 | −48.4375 | Si(7) | 0.6281 | −48.448 | Ge(7) | 0.6092 | −153.911 | Ge(7) | 0.6049 | −153.922 |
| C(8) | −0.6666 | −14.7584 | C(8) | −0.6739 | −14.7642 | C(8) | −0.6311 | −14.6862 | C(8) | −0.6313 | −14.6887 |
| C(9) | −0.4844 | −14.7239 | C(9) | −0.5115 | −14.7378 | C(9) | −0.4373 | −14.6715 | C(9) | −0.4596 | −14.6975 |
| Si(10) | 0.4601 | −48.4976 | Si(10) | 0.4694 | −48.5212 | Ge(10) | 0.4184 | −153.917 | G(10) | 0.3929 | −153.941 |
| Si(11) | 0.3110 | −48.583 | Si(11) | 0.4335 | −48.5485 | Ge(11) | 0.2338 | −153.986 | Ge(11) | 0.3472 | −153.99 |
| C(12) | −0.4512 | −14.7206 | C(12) | −0.4765 | −14.7486 | C(12) | −0.4001 | −14.6755 | C(12) | −0.4081 | −14.7029 |
| Si(13) | 0.4501 | −48.5069 | Si(13) | 0.5577 | −48.5043 | Ge(13) | 0.3916 | −153.938 | Ge(13) | 0.4952 | −153.976 |
| C(14) | −0.4844 | −14.7239 | C(14) | −0.5115 | −14.7378 | C(14) | −0.4373 | −14.6715 | C(14) | −0.4596 | −14.6975 |
| C(15) | −0.3158 | −14.7558 | C(15) | −0.4042 | −14.7189 | C(15) | −0.2627 | −14.7083 | C(15) | −0.3785 | −14.6938 |
| Si(16) | 0.4501 | −48.5069 | Si(16) | 0.5577 | −48.5043 | Ge(16) | 0.3916 | −153.938 | Ge(16) | 0.4952 | −153.976 |
| C(17) | −0.3491 | −14.7754 | C(17) | −0.4122 | −14.7179 | C(17) | −0.2887 | −14.7187 | C(17) | −0.3626 | −14.677 |
| C(18) | −0.3491 | −14.7754 | C(18) | −0.4122 | −14.7179 | C(18) | −0.2887 | −14.7187 | C(18) | −0.3626 | −14.677 |
| | | | H(19) | −0.1245 | −1.2466 | | | | H(19) | −0.0808 | −1.2055 |
| | | | H(20) | −0.1254 | −1.2421 | | | | H(20) | −0.0793 | −1.1995 |
| | | | H(21) | −0.1245 | −1.2466 | | | | H(21) | −0.0808 | −1.2055 |
| | | | H(22) | 0.0330 | −1.1770 | | | | H(22) | 0.0505 | −1.1604 |
| | | | H(23) | 0.0332 | −1.1951 | | | | H(23) | 0.0540 | −1.1689 |
| | | | H(24) | 0.0332 | −1.1951 | | | | H(24) | 0.0540 | −1.1689 |

| Sn-C_NC | | | H@Sn-C_NC | | | Pb-C_NC | | | H@Pb-C_NC | | |
|---|---|---|---|---|---|---|---|---|---|---|---|
| Atom | $Q$ | $E_p$ | Atom | $Q$ | $E_p$ | Atom | $Q$ | $E_p$ | Atom | $Q$ | $E_p$ |
| Sn(1) | 0.3787 | −284.1396 | Sn(1) | 0.5724 | −284.114 | Pb(1) | 0.4641 | −1.6181 | Pb1 | 0.5181 | −1.6193 |
| Sn(2) | 0.6382 | −283.7272 | Sn(2) | 0.6699 | −283.74 | Pb(2) | 0.1438 | −1.5339 | Pb2 | 0.1552 | −1.5519 |
| C(3) | −0.6662 | −14.73518 | C(3) | −0.6531 | −14.7512 | C(3) | −0.9130 | −14.787 | C3 | −0.9228 | −14.8081 |
| Sn(4) | 0.6680 | −284.0589 | Sn(4) | 0.6423 | −284.081 | Pb(4) | 0.8615 | −1.5799 | Pb4 | 0.8515 | −1.5982 |
| Sn(5) | 0.4801 | −284.1451 | Sn(5) | 0.6068 | −284.111 | Pb(5) | 0.6254 | −1.6217 | Pb5 | 0.6371 | −1.6140 |
| C(6) | −0.6210 | −14.7433 | C(6) | −0.6554 | −14.7892 | C(6) | −0.8941 | −14.7884 | C6 | −0.9032 | −14.8208 |
| Sn(7) | 0.8287 | −284.0484 | Sn(7) | 0.8584 | −284.056 | Pb(7) | 0.7935 | −1.5598 | Pb7 | 0.7357 | −1.5792 |
| C(8) | −0.7438 | −14.6500 | C(8) | −0.7563 | −14.6564 | C(8) | 0.0335 | −14.76 | C8 | 0.0352 | −14.778 |
| C(9) | −0.6772 | −14.7617 | C(9) | −0.6950 | −14.7774 | C(9) | −0.7484 | −14.8077 | C9 | −0.7587 | −14.8172 |

Table 1. (cont.)

| Sn-C_NC | | | H@Sn-C_NC | | | Pb-C_NC | | | H@Pb-C_NC | | |
|------|------|------|------|------|------|------|------|------|------|------|------|
| Atom | $Q$ | $E_p$ | Atom | $Q$ | $E_p$ | Atom | $Q$ | $E_p$ | Atom | $Q$ | $E_p$ |
| Sn(10) | 0.6680 | −284.0589 | Sn(10) | 0.6423 | −284.081 | Pb(10) | 0.8615 | −1.5799 | Pb10 | 0.8530 | −1.5981 |
| Sn(11) | 0.3787 | −284.1396 | Sn(11) | 0.5724 | −284.114 | Pb(11) | 0.4641 | −1.6181 | Pb11 | 0.5203 | −1.6191 |
| C(12) | −0.6210 | −14.7433 | C(12) | −0.6554 | −14.7892 | C(12) | −0.8941 | −14.7884 | C12 | −0.9039 | −14.8207 |
| Sn(13) | 0.6552 | −284.0813 | Sn(13) | 0.7660 | −284.101 | Pb(13) | 0.6859 | −1.5973 | Pb13 | 0.8239 | −1.6032 |
| C(14) | −0.6772 | −14.7617 | C(14) | −0.6950 | −14.7774 | C(14) | −0.7484 | −14.8077 | C14 | −0.7586 | −14.8172 |
| C(15) | −0.4494 | −14.7758 | C(15) | −0.5776 | −14.7784 | C(15) | −0.3692 | −14.7679 | C15 | −0.6837 | −14.8006 |
| Sn(16) | 0.6552 | −284.0813 | Sn(16) | 0.7660 | −284.101 | Pb(16) | 0.6859 | −1.5973 | Pb16 | 0.8243 | −1.6030 |
| C(17) | −0.4476 | −14.7665 | C(17) | −0.5268 | −14.7389 | C(17) | −0.526 | −14.7799 | C17 | −0.7146 | −14.7992 |
| C(18) | −0.4476 | −14.7665 | C(18) | −0.5268 | −14.7389 | C(18) | −0.526 | −14.7799 | C18 | −0.7128 | −14.7992 |
| | | | H(19) | −0.1566 | −1.23558 | | | | H19 | −0.0690 | −1.0892 |
| | | | H(20) | −0.1507 | −1.22487 | | | | H20 | −0.0674 | −1.0899 |
| | | | H(21) | −0.1566 | −1.23558 | | | | H21 | −0.0743 | −1.0893 |
| | | | H(22) | 0.0323 | −1.20447 | | | | H22 | 0.2066 | −1.0660 |
| | | | H(23) | 0.0383 | −1.20075 | | | | H23 | 0.2043 | −1.0864 |
| | | | H(24) | 0.0383 | −1.20075 | | | | H24 | 0.2036 | −1.0864 |

Table 1 has shown the nuclear quadrupole resonance for H-grabbing on the nano-carbides of Si-C_NC, Ge-C_NC, Sn-C_NC or Pb-C_NC and formation of H@Si-C_NC, H@Ge-C_NC, H@Sn-C_NC, H@Pb-C_NC clusters.



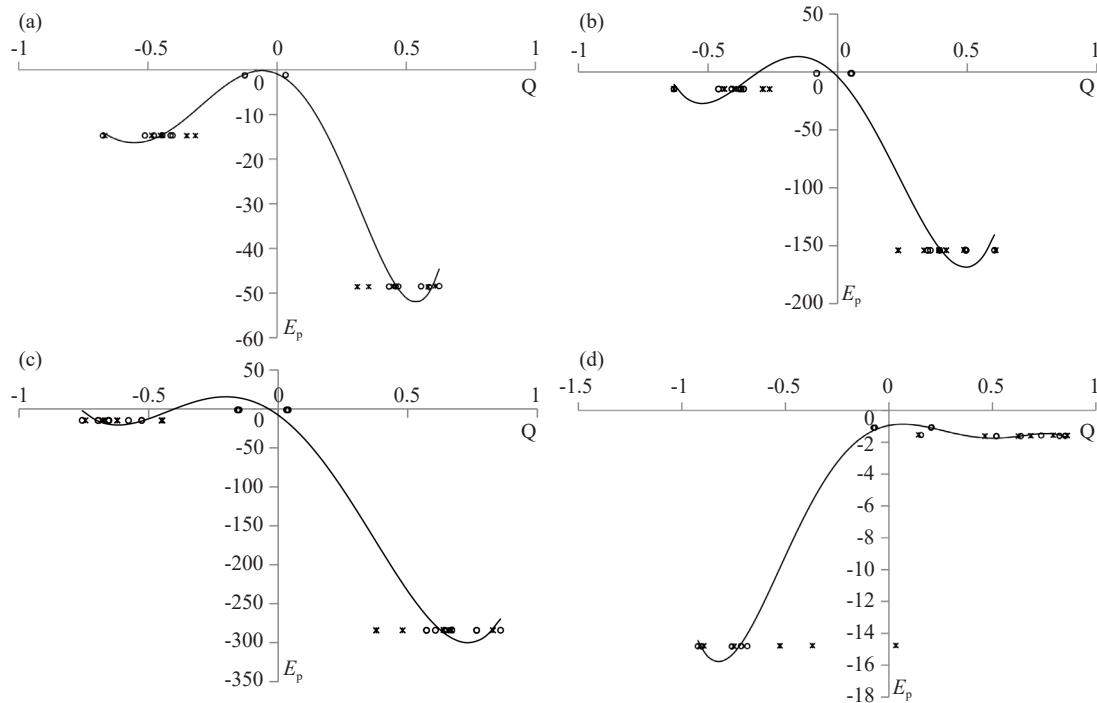**Figure 3.** "NQR" parameters for (a) H@Si-C_NC, (b) H@Ge-C_NC, (c) H@Sn-C_NC, and (d) H@Pb-C_NC clusters

Furthermore, the electric potential of nuclear quadrupole resonance method versus Bader charge for H-grabbing on the Si-C_NC, Ge-C_NC, Sn-C_NC or Pb-C_NC by "CAM-B3LYP/EPR-III, 6-311+G (d, p), LANL2DZ" theoretical level has been shown (Figure 3a-d). As the number of calculation studies related to metals and metalloids has been enhancing, the "LANL2DZ" basis set has become one of the most common basis sets for metal and metalloid complexes among others. "EPR-III" is a triple zeta basis set consisting of diffuse functions, double d-polarizations and a single set of f-polarization functions. In this case, the s-part is developed to better illustrate the nuclear zone.

It has been observed the impact of the binding between hydrogen atoms with C, Si, Ge, Sn and Pb in the H@Si-C_NC, H@Ge-C_NC, H@Sn-C_NC, H@Pb-C_NC during H-grabbing through "NQR" analysis (Figure 3a-d). The plots of H@Si-C_NC (Figure 3a), H@Ge-C_NC (Figure 3b), H@Sn-C_NC (Figure 3c), and H@Pb-C (Figure 3d), respectively, have illustrated the impact of H-grabbing on the Si-C_NC, Ge-C_NC, Sn-C_NC and Pb-C_NC clusters. It is suitable for the study of measured nanoclusters containing quadrupole nuclei where the characteristic NQR frequencies represent the fingerprints of these compounds. In several cases, $^{14}$N NQR can distinguish between the crystalline phases of hydrogenated surfaces. So, it can be stated that $^{14}$N NQR is a powerful contactless tool for detecting the appearance of H-grabbing with a possibility to distinguish clearly and quantitatively among different nanoclusters.


## 3.3 *Magnetism of H-adsorption on Si-C_NC, Ge-C_NC, Sn-C_NC, Pb-C_NC*

"NMR" parameters for certain atoms in the active site of H-grabbing on the Si-C_NC, Ge-C_NC, Sn-C_NC, Pb-C_NC through the linkage between H-atoms and nano-carbides towards forming H@Si-C_NC, H@Ge-C_NC, H@Sn-C_NC, H@Pb-C_NC hydrides have been measured in Table 2. The density functional theory (DFT) calculations have been executed using the Gaussian 16 package.[46]

Table 2. "NMR" parameters of H-grabbing on the Si-C_NC, Ge-C_NC, Sn-C_NC or Pb-C_NC clusters

| Si-C_NC | | | H@Si-C_NC | | | Ge-C_NC | | | H@Ge-C_NC | | |
|---|---|---|---|---|---|---|---|---|---|---|---|
| Atom | $\sigma_{iso}$ | $\sigma_{aniso}$ | Atom | $\sigma_{iso}$ | $\sigma_{aniso}$ | Atom | $\sigma_{iso}$ | $\sigma_{aniso}$ | Atom | $\sigma_{iso}$ | $\sigma_{aniso}$ |
| Si(1) | 1,852.8960 | 9,277.8581 | Si(1) | 652.0996 | 2,043.4448 | Ge(1) | 524.2652 | 4,076.8426 | Ge(1) | 1,685.9528 | 995.5874 |
| Si(2) | 707.1922 | 1,372.5500 | Si(2) | 578.8802 | 1,376.1814 | Ge(2) | 2,938.4569 | 1,816.3038 | Ge(2) | 2,046.7422 | 677.2387 |
| C(3) | 26.3336 | 1,184.7146 | C(3) | 328.7614 | 1,145.6732 | C(3) | 1,055.1306 | 1,882.3207 | C(3) | 45.4161 | 593.3670 |
| Si(4) | 396.8693 | 636.0558 | Si(4) | 939.4444 | 1,737.4509 | Ge(4) | 1,995.8705 | 1,646.8872 | Ge(4) | 1,943.3848 | 1,109.6931 |
| Si(5) | 751.2993 | 5,584.1673 | Si(5) | 787.0425 | 1,304.9949 | Ge(5) | 1,063.4297 | 2,074.3377 | Ge(5) | 2,694.1662 | 2,627.1478 |
| C(6) | 180.1857 | 6,093.0613 | C(6) | 1,995.0521 | 4,581.1275 | C(6) | 517.8104 | 2,231.1687 | C(6) | 398.1112 | 1,004.5925 |
| Si(7) | 44.5656 | 1,523.6745 | Si(7) | 112.7493 | 579.3102 | Ge(7) | 1,817.7074 | 1,660.1330 | Ge(7) | 1,618.7559 | 555.2137 |
| C(8) | 62.5710 | 392.1047 | C(8) | 269.5126 | 621.8678 | C(8) | 54.3886 | 222.9889 | C(8) | 6.1355 | 304.2995 |
| C(9) | 334.2540 | 1,328.9150 | C(9) | 624.3653 | 2,381.2166 | C(9) | 250.6261 | 776.3827 | C(9) | 73.4150 | 442.0441 |
| Si(10) | 396.8693 | 636.0558 | Si(10) | 939.4444 | 1,737.4509 | Ge(10) | 1,995.8705 | 1,646.8872 | G(10) | 1,943.3848 | 1,109.6931 |
| Si(11) | 1,852.8960 | 9,277.8581 | Si(11) | 652.0996 | 2,043.4448 | Ge(11) | 524.2652 | 4,076.8426 | Ge(11) | 1,685.9528 | 995.5874 |
| C(12) | 180.1857 | 6,093.0613 | C(12) | 1,995.0521 | 4,581.1275 | C(12) | 517.8104 | 2,231.1687 | C(12) | 398.1112 | 1,004.5925 |
| Si(13) | 758.7227 | 5,091.8836 | Si(13) | 428.6833 | 428.6833 | Ge(13) | 1,064.2837 | 1,824.8636 | Ge(13) | 2,199.6950 | 1,909.5554 |

**Table 2.** (cont.)

| | Si-C_NC | | | H@Si-C_NC | | | Ge-C_NC | | | H@Ge-C_NC | |
|---|---|---|---|---|---|---|---|---|---|---|---|
| Atom | $\sigma_{iso}$ | $\sigma_{aniso}$ | Atom | $\sigma_{iso}$ | $\sigma_{aniso}$ | Atom | $\sigma_{iso}$ | $\sigma_{aniso}$ | Atom | $\sigma_{iso}$ | $\sigma_{aniso}$ |
| C(14) | 334.2540 | 1,328.9150 | C(14) | 624.3653 | 2,381.2166 | C(14) | 250.6261 | 776.3827 | C(14) | 73.4150 | 442.0441 |
| C(15) | 215.4441 | 2,129.1385 | C(15) | 434.8456 | 933.7457 | C(15) | 451.4650 | 2,033.6451 | C(15) | 308.3324 | 606.6501 |
| Si(16) | 758.7227 | 5,091.8836 | Si(16) | 428.6833 | 678.2943 | Ge(16) | 1,064.2837 | 1,824.8636 | Ge(16) | 2,199.6950 | 1,909.5554 |
| C(17) | 6,842.2257 | 11,517.1989 | C(17) | 3.3059 | 424.8038 | C(17) | 2,301.7865 | 5,664.7386 | C(17) | 29.3094 | 277.5181 |
| C(18) | 6,842.2257 | 11,517.1989 | C(18) | 3.3059 | 424.8038 | C(18) | 2,301.7865 | 5,664.7386 | C(18) | 29.3094 | 277.5181 |
| | | | H(19) | 35.7119 | 53.7922 | | | | H(19) | 28.7663 | 15.3241 |
| | | | H(20) | 22.7277 | 19.1040 | | | | H(20) | 28.5430 | 18.0659 |
| | | | H(21) | 35.7119 | 53.7922 | | | | H(21) | 28.7663 | 15.3241 |
| | | | H(22) | 45.5793 | 57.7040 | | | | H(22) | 41.0031 | 48.3955 |
| | | | H(23) | 18.3406 | 13.9135 | | | | H(23) | 21.0924 | 11.7482 |
| | | | H(24) | 18.3406 | 13.9135 | | | | H(24) | 21.0924 | 11.7482 |

| | Sn-C_NC | | | H@Sn-C_NC | | | Pb-C_NC | | | H@Pb-C_NC | |
|---|---|---|---|---|---|---|---|---|---|---|---|
| Atom | $\sigma_{iso}$ | $\sigma_{aniso}$ | Atom | $\sigma_{iso}$ | $\sigma_{aniso}$ | Atom | $\sigma_{iso}$ | $\sigma_{aniso}$ | Atom | $\sigma_{iso}$ | $\sigma_{aniso}$ |
| Sn(1) | 3,852.4768 | 1,253.8614 | Sn(1) | 5,331.1122 | 3,908.8109 | Pb(1) | 8.3138 | 81.0012 | Pb(1) | 12.3612 | 13.2040 |
| Sn(2) | 4,488.4542 | 630.7182 | Sn(2) | 8,048.7803 | 12,679.4768 | Pb(2) | 21.0773 | 19.9446 | Pb(2) | 20.9858 | 15.8398 |
| C(3) | 692.2861 | 2,220.5600 | C(3) | 3,086.7050 | 9,101.5478 | C(3) | 337.2144 | 1,607.1525 | C(3) | 131.0567 | 958.8770 |
| Sn(4) | 4,033.8531 | 734.5909 | Sn(4) | 5,625.1352 | 9,355.5742 | Pb(4) | 1.8733 | 35.7403 | Pb(4) | 9.3660 | 21.0628 |
| Sn(5) | 3,660.3970 | 1,122.0832 | Sn(5) | 7,373.9159 | 4,446.7111 | Pb(5) | 33.6067 | 62.8027 | Pb(5) | 12.5136 | 24.9133 |
| C(6) | 117.5385 | 651.1418 | C(6) | 1,601.6375 | 4,860.7895 | C(6) | 615.7565 | 2,721.2686 | C(6) | 448.3251 | 912.9272 |
| Sn(7) | 3,631.0020 | 1,598.1063 | Sn(7) | 11,387.7893 | 22,754.5333 | Pb(7) | 19.1565 | 58.8387 | Pb(7) | 20.4001 | 17.7409 |
| C(8) | 114.3168 | 171.0993 | C(8) | 6,947.4689 | 10,490.2518 | C(8) | 184.8183 | 320.2073 | C(8) | 510.5573 | 949.4451 |
| C(9) | 192.3590 | 634.9115 | C(9) | 419.8777 | 2,370.5045 | C(9) | 61.9853 | 889.5642 | C(9) | 113.4349 | 520.4584 |
| Sn(10) | 4,033.8531 | 734.5909 | Sn(10) | 5,625.1352 | 9,355.5742 | Pb(10) | 1.8733 | 35.7403 | Pb(10) | 9.2549 | 21.0870 |
| Sn(11) | 3,852.4768 | 1,253.8614 | Sn(11) | 5,331.1122 | 3,908.8109 | Pb(11) | 8.3138 | 81.0012 | Pb(11) | 12.2325 | 13.1823 |
| C(12) | 117.5385 | 651.1418 | C(12) | 1,601.6375 | 4,860.7895 | C(12) | 615.7565 | 2,721.2686 | C(12) | 446.5082 | 899.4323 |
| Sn(13) | 4,274.5080 | 544.9696 | Sn(13) | 2,735.2331 | 3,523.3606 | Pb(13) | 17.5248 | 27.0793 | Pb(13) | 8.0973 | 13.0066 |
| C(14) | 192.3590 | 634.9115 | C(14) | 419.8777 | 2,370.5045 | C(14) | 61.9853 | 889.5642 | C(14) | 115.2409 | 523.1188 |
| C(15) | 677.3063 | 2,314.0820 | C(15) | 1,362.9700 | 2,901.5605 | C(15) | 492.2542 | 3,669.8947 | C(15) | 266.7875 | 599.4562 |
| Sn(16) | 4,274.5080 | 544.9696 | Sn(16) | 2,735.2331 | 3,523.3606 | Pb(16) | 17.5248 | 27.0793 | Pb(16) | 8.0859 | 12.8627 |
| C(17) | 992.3714 | 2,612.5933 | C(17) | 125.3188 | 949.5305 | C(17) | 523.3055 | 3,890.6558 | C(17) | 109.6002 | 357.9518 |
| C(18) | 992.3714 | 2,612.5933 | C(18) | 125.3188 | 949.5305 | C(18) | 523.3055 | 3,890.6558 | C(18) | 109.5379 | 356.4523 |
| | | | H(19) | 29.6065 | 44.0962 | | | | H(19) | 24.8456 | 9.3054 |
| | | | H(20) | 24.6953 | 11.3083 | | | | H(20) | 23.6407 | 8.6042 |
| | | | H(21) | 29.6065 | 44.0962 | | | | H(21) | 24.5059 | 8.9632 |
| | | | H(22) | 60.6118 | 70.1035 | | | | H(22) | 39.9395 | 42.2828 |
| | | | H(23) | 0.8243 | 61.1416 | | | | H(23) | 18.3117 | 16.5055 |
| | | | H(24) | 0.8243 | 61.1416 | | | | H(24) | 18.3067 | 16.3958 |
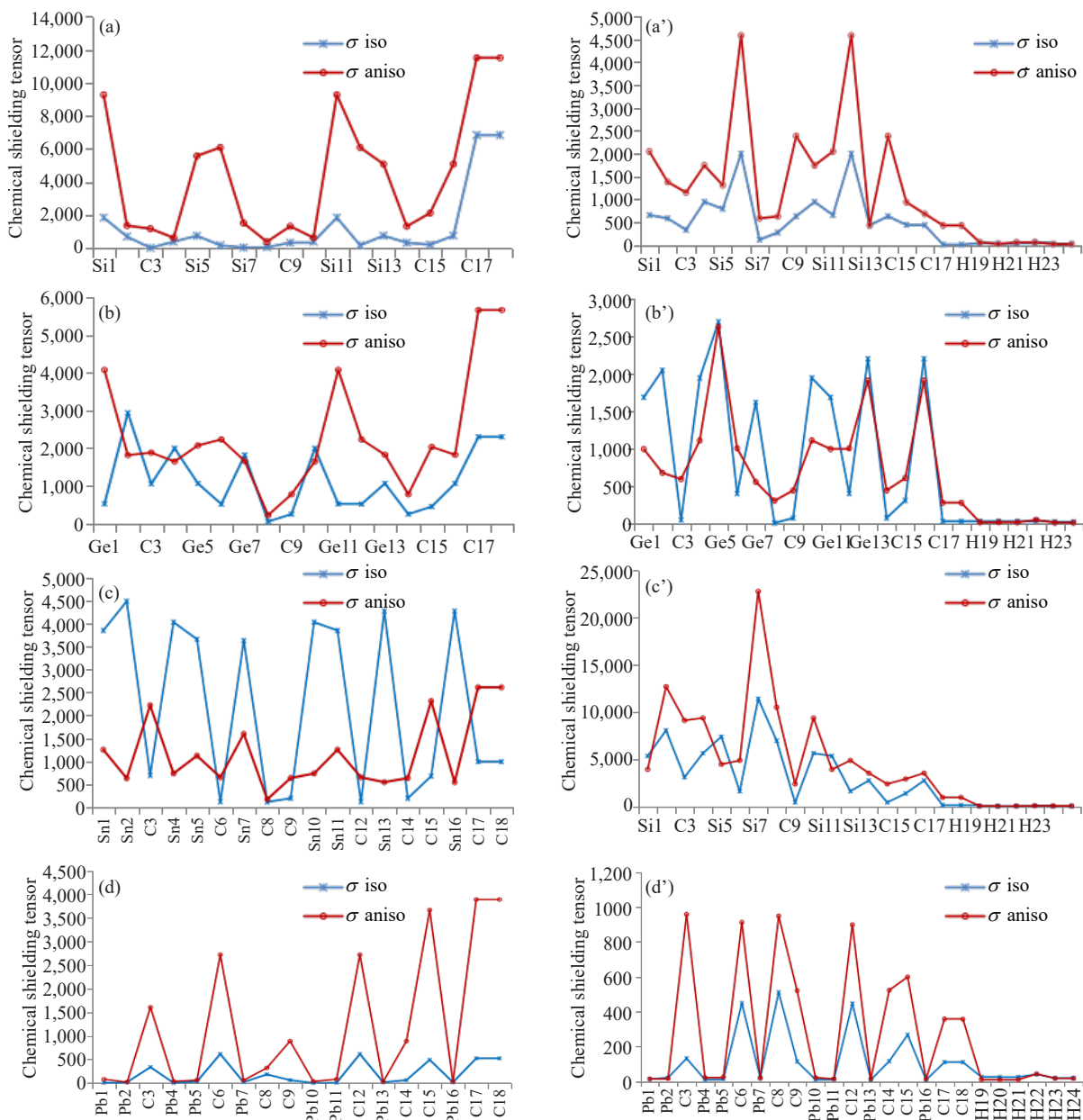
**Figure 4.** Isotropic ($\sigma_{iso}$) and anisotropy ($\sigma_{aniso}$) tensors derived from NMR spectrums for (a) Si-C_NC, (a') H@Si-C_NC, (b) Ge-C_NC, (b') H@Ge-C_NC, (c) Sn-C_NC, (c') H@Sn-C_NC, (d) Pb-C_NC and (d') H@Pb-C_NC clusters

"NMR" graphs in Figure 4 (a-d, a'-d') have indicated the similar chemical shielding attitude of isotropic and anisotropy factors of Si-C_NC, Ge-C_NC, Sn-C_NC, Pb-C_NC and H@Si-C_NC, H@Ge-C_NC, H@Sn-C_NC, H@Pb-C_NC clusters with several sharp peaks related to C, Si, Ge, Sn, Pb "adsorbent" and H-atoms "adsorbate" in the active zones.[53,54]

Adsorption "NMR" graphs of Si1, Si5, Si11, C6, C17, C18 for SiC (Figure 4a) and C6, C12 for H@SiC (Figure 4a'); Ge1, Ge11, C17, C18 for GeC (Figure 4b) and Ge2, Ge5, Ge7, Ge10, Ge13, Ge16 for H@GeC (Figure 4b'); Sn2, Sn4, Sn5, Sn7, Sn10, Sn11, Sn13, Sn16 for SnC (Figure 4c) and Sn2 for H@SnC (Figure 4c'); C3, C6, C12, C15, C17, C18 for PbC (Figure 4d) and C3, C6, C8, C12 for H@PbC (Figure 4d'), respectively have been indicated.

## 3.4 Vibrations of H-adsorption onto Si-C_NC, Ge-C_NC, Sn-C_NC, Pb-C_NC

Concerning adsorption process, the thermodynamic parameters were measured for H-grabbing on the nano-carbides of Si-C_NC, Ge-C_NC, Sn-C_NC, Pb-C_NC as the gas sensors which might be suitable for H-storing (Table 3).

**Table 3.** The thermodynamic properties of Si-C_NC, H@Si-C_NC, Ge-C_NC, H@Ge-C_NC, Sn-C_NC, H@Sn-C_NC, Pb-C_NC and H@Pb-C_NC complexes

| Nanocone and H-adsorption | $\Delta E^{\circ} \times 10^{-4}$ (kcal/mol) | $\Delta H^{\circ} \times 10^{-4}$ (kcal/mol) | $\Delta G^{\circ} \times 10^{-4}$ (kcal/mol) | $S^{\circ}$ (Cal/K·mol) | Dipole moment (Debye) | Convergence | k-point grid |
|---|---|---|---|---|---|---|---|
| Si-C_NC | -182.7474 | -182.7474 | -182.7514 | 134.576 | 4.1234 | 0.7415D-08 | 2.0062 |
| H@Si-C_NC | -182.9776 | -182.9775 | -182.9815 | 132.507 | 2.3194 | 0.7508D-08 | 2.0154 |
| Ge-C_NC | -1,180.6421 | -1,180.6421 | -1,180.6465 | 148.277 | 3.3993 | 0.5017D-08 | 2.0007 |
| H@Ge-C_NC | -1,180.8751 | -1,180.8750 | -1,180.8798 | 161.024 | 1.4991 | 0.5591D-08 | 2.0021 |
| Sn-C_NC | -3,390.0971 | -3,390.0970 | -3,390.1014 | 147.503 | 3.0569 | 0.7533D-08 | 2.0003 |
| H@Sn-C_NC | -3,390.3269 | -3,390.3269 | -3,390.3316 | 157.153 | 2.1738 | 0.7927D-08 | 2.0009 |
| Pb-C_NC | -23.3096 | -23.3095 | -23.3132 | 123.440 | 8.6603 | 0.8073D-08 | 1.9967 |
| H@Pb-C_NC | -23.5365 | -23.5365 | -23.5405 | 136.838 | 3.1099 | 0.8236D-08 | 2.0001 |

Furthermore, the "IR" spectra for H-grabbing on the Si-C_NC, Ge-C_NC, Sn-C_NC or Pb-C_NC clusters have been seen in Figure 5 (a-d, a'-d'). The curve of Figure 5 (a) and (a') has been seen in the frequency range between 500-2,500 cm$^{-1}$ for the complex of Si-C_NC and H@Si-C_NC with pointed peaks near 815.93 cm$^{-1}$ and 227.03 cm$^{-1}$, respectively. The graph of Figure 5 (b) and (b') has been found in the frequency range between 500-1,000 cm$^{-1}$ for the complex of Ge-C_NC and H@Ge-C_NC with pointed peaks near 588.37 cm$^{-1}$ and 777.77 cm$^{-1}$, respectively. The curve of Figure 5 (c) and (c') has been indicated in the frequency range between 250-1,250 cm$^{-1}$ for the complex of Sn-C_NC and H@Sn-C_NC with pointed peaks near 761.38 cm$^{-1}$ and 393.08 cm$^{-1}$, respectively. The curve of Figure 5 (d) and (d') has been shown in the frequency range around 1,500-2,500 cm$^{-1}$ for the complex of Pb-C_NC and H@Pb-C_NC with pointed peaks near 182.37 cm$^{-1}$ and 1,515.14 cm$^{-1}$, respectively.

H-grabbing on the Si-C_NC, Ge-C_NC, Sn-C_NC or Pb-C_NC clusters is approved by the $\Delta E^{\circ}_{ads}$ amounts as formula:

$$\Delta E^{\circ}_{ads} = \Delta E^{\circ}_{H \to X\text{-}C\_NC} - (\Delta E^{\circ}_{H} + \Delta E^{\circ}_{X\text{-}C\_NC}); (X = Si, Ge, Sn, Pb) \tag{5}$$

Besides, the alterations of $\Delta H^{\circ}_{ads}$ among H-grabbing on the Si-C_NC, Ge-C_NC, Sn-C_NC or Pb-C_NC clusters were measures regarding non-covalent binding extracted from interatomic interactions between H-atoms and nano-carbides of Si-C_NC, Ge-C_NC, Sn-C_NC and Pb-C_NC and covalent binding extracted from intra-atomic interactions between C, Si, Ge, Sn, Pb in the nanocone structures (Table 3). As a matter of fact, Si-C_NC, Ge-C_NC, Sn-C_NC or Pb-C_NC have greater interaction energy from Van der Waals' forces with H-atoms that can cause them to be much more resistant (Figure 6). The H-grabbing band reflects the saturated hydrogen content on the surface of nanoclusters.

By combining these observed and calculated results, the configurations of hydrogen atoms at the interface of the nanocluster can be discussed.
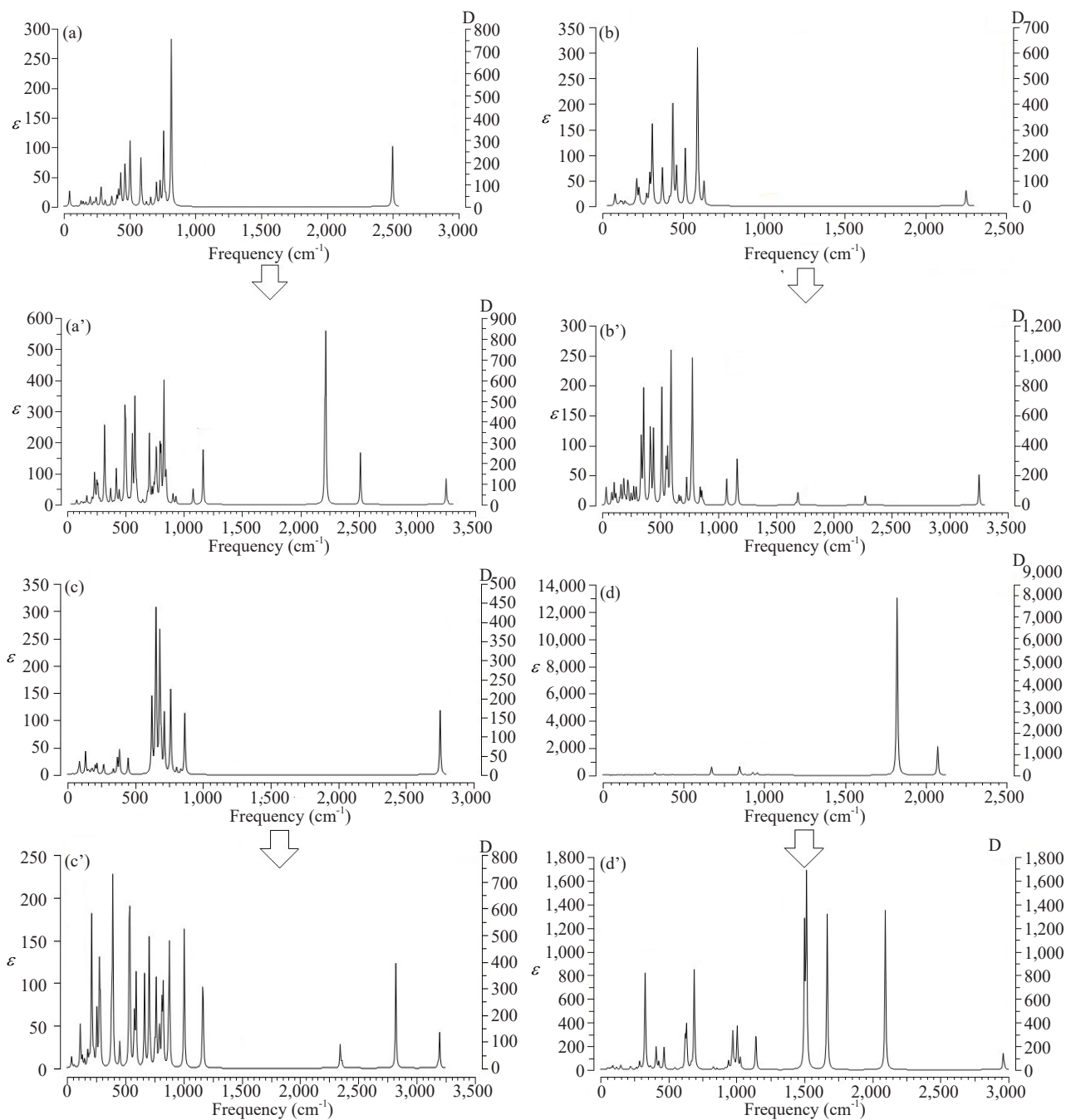


**Figure 5.** "IR" spectra for (a) Si-C_NC, (a') H@Si-C_NC, (b) Ge-C_NC, (b') H@Ge-C_NC, (c) Sn-C_NC, (c') H@Sn-C_NC, (d) Pb-C_NC and (d') H@Pb-C_NC complexes as the selective gas detectors
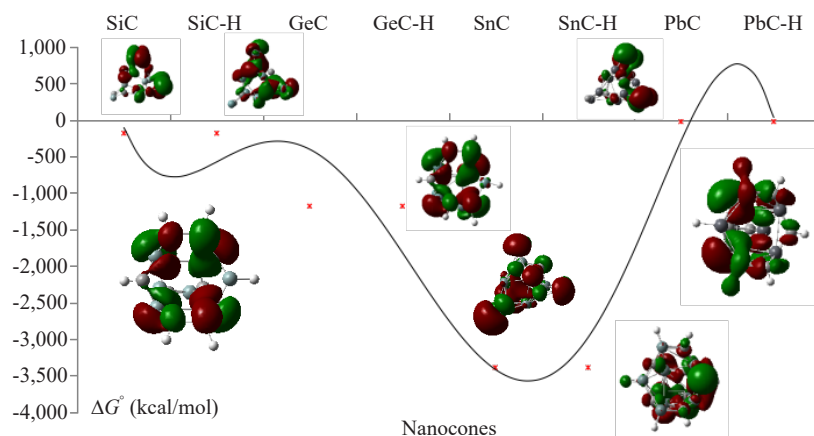
**Figure 6.** The alterations of Gibbs free energy ($\Delta G^{\circ}_{ads}$) for H-grabbing onto Si-C_NC, Ge-C_NC, Sn-C_NC and Pb-C_NC clusters

And $\Delta G^{\circ}_{ads}$ is evaluated as the following formula:

$$\Delta G^{\circ}_{ads} = \Delta G^{\circ}_{H@\,X\text{-}C\_NC} - (\Delta G^{\circ}_{H} + \Delta G^{\circ}_{X\text{-}C\_NC}); \; (X = Si, Ge, Sn, Pb) \tag{6}$$

All the computed amounts of $\Delta G^{\circ}_{ads}$ are close (Table 3) that explains the coherence of the measured values by all methods and the validity of the computational methods and force fields (Figure 6).

Table 3 and Figure 6 have displayed that H@Si-C_NC, H@Ge-C_NC, H@Sn-C_NC, H@Pb-C_NC clusters have the greatest interval of Gibbs free energy adsorption with which describes the alterations between Gibbs free energy of input compounds ($\Delta G^{\circ}_{H}$) and ($\Delta G^{\circ}_{Si\text{-}C\_NC}$, $\Delta G^{\circ}_{Ge\text{-}C\_NC}$, $\Delta G^{\circ}_{Sn\text{-}C\_NC}$, $\Delta G^{\circ}_{Pb\text{-}C\_NC}$) and product compounds ($\Delta G^{\circ}_{H@Si\text{-}C\_NC}$, $\Delta G^{\circ}_{H@Ge\text{-}C\_NC}$, $\Delta G^{\circ}_{H@Sn\text{-}C\_NC}$, $\Delta G^{\circ}_{H@Pb\text{-}C\_NC}$) based on the polarizability factor.

Therefore, it is supposed that Si-C_NC, Ge-C_NC, Sn-C_NC or Pb-C_NC contain sufficient productivity for H-grabbing on the mentioned nano-carbides through charge transfer from H-atoms to C, Si, Ge, Sn or Pb due to intra-atomic and interatomic interactions.

# 4. Conclusions

In summary, H-grabbing on the nano-carbides of Si-C_NC, Ge-C_NC, Sn-C_NC and Pb-C_NC was investigated by first-principles calculations. The alterations of charge density illustrated a remarkable charge transfer towards Si-C_NC, Ge-C_NC, Sn-C_NC or Pb-C_NC which might play the electron acceptor roles while H-atoms act as the stronger electron donors through adsorption on the Si-C_NC, Ge-C_NC, Sn-C_NC or Pb-C_NC. As a matter of fact, Si-C_NC, Ge-C_NC, Sn-C_NC or Pb-C_NC have greater interaction energy from Van der Waals' forces with H-atoms that can cause them to be much more resistant. Besides, thermodynamic parameters describing H-grabbing on the nano-carbides of Si-C_NC, Ge-C_NC, Sn-C_NC or Pb-C_NC have been investigated, including internal process of the adsorbent-adsorbate system. Thermodynamic parameters have constructed a detailed molecular model for atom-atom interactions and a distribution of point charges which can be utilized to reproduce the polarity of the solid material and the adsorbing molecules. Today, it is crucial to distinguish the potential of hydrogen technologies and bring up all perspectives of their performance, from technological advances to economic and social effects. The authors intend to pursue research on sustainability and clean energy subjects towards finding new solutions for reducing the global dependency on fossil fuels.

# Acknowledgements

## Conflict of interest

The author declares that they have no conflict of interest.

## References

[1] Seminario-Córdova, R.; Rojas-Ortega, R. Renewable energy sources and energy production: A bibliometric analysis of the last five years. *Sustainability* **2023,** *15*, 10499.

[2] Olabi, A. G.; Sayed, E. T. Developments in hydrogen fuel cells. *Energies* **2023,** *16*, 2431.

[3] Pavlenko, V. I.; Cherkashina, N. I.; Edamenko, O. D.; Yastrebinsky, R. N.; Noskov, A. V.; Prokhorenkov, D. S.; Gorodov, A. I.; Piskareva, A. O. Synthesis and characterization of Silicon-Carbon powder and its resistance to electron irradiation. *J. Compos. Sci.* **2023,** *7*, 340.

[4] Das,V.; Padmanaban, S.; Venkitusamy, K.; Selvamuthukumaran, R.; Blaabjerg, F.; Siano, P. Recent advances and challenges of fuel cell based power system architectures and control-A review. *Renew. Sustain. Energy Rev.* **2017,** *73*, 10-18.

[5] Mollaamin, F. Competitive intracellular hydrogen-nanocarrier among aluminum, carbon, or silicon implantation: A novel technology of eco-friendly energy storage using research density functional theory. *Russ. J. Phys. Chem. B.* **2024,** *18*, 805-820.

[6] Feng, X.; Sun, L.; Wang, W.; Zhao, Y.; Shi, J. W. Hybrid energy storage system and management strategy for motor drive with high torque overload. *Sep. Purif. Technol.* **2023,** *324*, 124520.

[7] Strobel, R.; Garche, J.; Moseley, P. T.; Jorissen, L.; Wolf, G. Hydrogen storage by carbon materials. *J. Power Sources.* **2006,** *159*, 781-801.

[8] Utomo, O.; Abeysekera, M.; Ugalde-Loo, C. E. Optimal operation of a hydrogen storage and fuel cell coupled integrated energy system. *Sustainability* **2021,** *13*, 3525.

[9] Nqodi, A.; Mosetlhe, T. C.; Yusuff, A. A. Advances in hydrogen-powered trains: A brief report. *Energies* **2023,** *16*, 6715.

[10] Jeerapan, I.; Sempionatto, J. R.; Wang, J. On-body bioelectronics: Wearable biofuel cells for bioenergy harvesting and self-powered biosensing. *Adv. Funct. Mater.* **2020,** *30*, 1906243.

[11] Caban, J.; Małek, A.; Kroczyński, D. A method for assessing the technical condition of traction batteries using the metalog family of probability distributions. *Energies* **2024,** *17*, 3096.

[12] Hao, S.; Sun, X.; Zhang, H.; Zhai, J.; Dong, S. Recent development of biofuel cell based self-powered biosensors. *J. Mater. Chem. B.* **2020,** *8*, 3393-3407.

[13] Kakoulaki, G.; Kougias, I.; Taylor, N.; Dolci, F.; Moya, J.; Jäger-Waldau, A. Green hydrogen in Europe-A regional assessment: Substituting existing production with electrolysis powered by renewables. *Energy Convers. Manag.* **2020,** *228*, 113649.

[14] Zhao, Y.; Kim, Y. H.; Dillon, A. C.; Heben, M. J; Zhang, S. B. Ab initio design of Ca-decorated organic frameworks for high capacity molecular hydrogen storage with enhanced binding. *Phys. Rev. Lett.* **2005,** *95*, 155504.

[15] Yang, F. H.; Lachawiec, A. J.; Yang, R. T. Hydrogen sorption on palladium-doped sepiolite-derived carbon nanofibers. *J. Phys. Chem. B.* **2006,** *110*, 6236-6244.

[16] Novoselov, K. S.; Geim, A. K.; Morozov, S. V.; Jiang, D.; Zhang, Y.; Dubonos, S. V.; Grigorieva, I. V.; Firsov, A. A. Electric field effect in atomically thin carbon films. *Science* **2004,** *306*, 666-669.

[17] Grishin, M. V.; Gatin, A. K.; Sarvadii, S. Y.; Slutskii, V. G.; Kharitonov, V. A. Quantum chemical simulation of reactions involved in electrically enhanced reduction of nickel and copper nanooxides with carbon monoxide. *Russ. J. Phys. Chem. B.* **2024,** *18*, 1275-1278.

[18] Castro Neto, A. H.; Guinea, F.; Peres, N. M. R.; Novoselov, K. S.; Geim, A. K. The electronic properties of graphene. *Rev. Mod. Phys.* **2009,** *81*, 109-162.

[19] Mak, K. F.; Lee, C.; Hone, J.; Shan, J.; Heinz, T. F. Atomically thin $MoS_2$: a new direct-gap semiconductor. *Phys. Rev. Lett.* **2012,** *105*, 136805-136807.

[20] Radisavljevic, B.; Radenovic, A.; Brivio, J.; Giacometti, V.; Kis, A. Single-layer $MoS_2$ transistors. *Nat. Nanotechnol.* **2022,** *6*, 147-150.

[21] Rodin, S.; Carvalho, A.; Castro Neto, A. H. Strain-induced gap modification in black phosphorus. *Phys. Rev. Lett.*

**2014,** *112*, 176801-176803.

[22] Balitskii, A. I.; Abramek, K. F.; Osipowicz, T. K.; Eliasz, J. J.; Balitska, V. O.; Kochmański, P.; Prajwowski, K.; Mozga, L. S. Hydrogen-containing "green" Fuels influence on the thermal protection and formation of wear processes components in compression-ignition engines modern injection system. *Energies* **2023,** *16*, 3374.

[23] Fei, R.; Faghaninia, A.; Soklaski, R.; Yan, J. A.; Lo, C.; Yang, L. Enhanced thermoelectric efficiency via orthogonal electrical and thermal conductances in phosphorene. *Nano Lett*. **2014,** *14*, 6393-6399.

[24] Ramasubramaniam, A.; Muniz, A. R. Ab initio studies of thermodynamic and electronic properties of phosphorene nanoribbons. *Phys. Rev. B*. **2014,** *90*, 085424-085429.

[25] Yan, Z.; Bai, Y.; Sun, L. Adsorption of thiophene and SOx molecules on Cr-doped and Ti-doped graphene nanosheets: a DFT study. *Mater. Res. Expres*. **2019,** *6*, 2019.

[26] Zhao, G.; Nielsen, E. R. *Social Impact Assessment of BIG HIT: A Report into the Societal Impact of the Project*; Department of Energy Conversion and Storage, Technical University of Denmark: Kongens Lyngby, Denmark, 2018.

[27] Pedicini, R. Special issue "hydrogen storage and fuel cells: Materials, characterization and applications". *Materials* **2022,** *15*, 423.

[28] Javan, M. B. Electronic and magnetic properties of monolayer SiC sheet doped with 3d-transition metals. *J. Magn. Magn. Mater*. **2016,** *401*, 656-66.

[29] Tatarewicz, I.; Skwierz, S.; Lewarski, M.; Jeszke, R.; Pyrka, M.; Sekuła, M. Mapping the future of green hydrogen: Integrated analysis of Poland and the EU's development pathways to 2050. *Energies* **2023,** *16*, 6261.

[30] Utamuradova, Sh. B.; Matchonov, Kh. J.; Khamdamov, J. J.; Utemuratova, Kh. Y. X-ray diffraction study of the phase state of silicon single crystals doped with manganese. *New Mater. Compd. Appl*. **2023,** *7*, 93-99.

[31] Utamuradova, Sh. B.; Daliev, Sh. Kh.; Bokiev, B. R.; Zarifbayev, J. Sh. X-ray spectroscopy of silicon doped with germanium atoms. *Adv. Phys. Res*. **2024,** *6*, 211-218.

[32] Abdullayeva, L. K.; Hasanov, M. H. Investigation of the role of metal in non-alloy metal-semiconductor (Si) contact. *New Mater. Compd. Appl*. **2024,** *8*, 135-141.

[33] Mollaamin, F.; Monajjemi, M. Nanomaterials for sustainable energy in hydrogen-fuel cell: Functionalization and characterization of carbon nano-semiconductors with silicon, germanium, tin or lead through density functional theory study. *Russ. J. Phys. Chem. B* **2024,** *18*, 607-623.

[34] Sokurov, A. A.; Rekhviashvili, S. S. Noncovalent interaction of carbon, silicon, and germanium atoms. *Russ. J. Phys. Chem. B*. **2024,** *18*, 1241-1248.

[35] Zolotarev, K. V.; Mikhailov, A. N.; Nakhod, V. I.; Tikhonova, E. G.; Mikhailova, M. V. Characterization and in vivo toxicity assay of uncoated silicon nanoparticles. *New Mater. Compd. Appl*. **2024,** *8*, 162-170.

[36] Kresse, G.; Furthmüller, J. Efficient iterative schemes for ab initio total-energy calculations using a plane-wave basis set. *Phys. Rev. B*. **1996,** *54*, 11169-11186.

[37] Perdew, J. P.; Burke, K.; Ernzerhof, M. Generalized gradient approximation made simple. *Phys. Rev. Lett*. **1996,** *77*, 3865-3868.

[38] Kresse, G.; Joubert, D. From ultrasoft pseudopotentials to the projector augmented-wave method. *Phys. Rev. B*. **1999,** *59*, 1758-1775.

[39] Zhang, X.; Tang, Y.; Zhang, F.; Lee, C. S. A novel aluminum-graphite dual-ion battery. *Adv. Energy Mater*. **2016,** *6*, 1502588.

[40] El-Eskandarany, M. S.; Ali, N.; Al-Ajmi, F.; Banyan, M.; Al-Duweesh, A. A. Hydrogen storage behavior and performance of multiple cold-rolled $MgH_2/Nb_2O_5$ nanocomposite Powders. *Processes*. **2022,** *10*, 1017.

[41] Cetinkaya, S. A.; Disli, T.; Soyturk, G.; Kizilkan, O.; Colpan, C. O. A review on thermal coupling of metal hydride storage tanks with fuel cells and electrolyzers. *Energies*. **2023,** *16*, 341.

[42] Bai, X. S.; Yang, W. W.; Tang, X. Y.; Dai, Z. Q.; Yang, F. S. Parametric optimization of coupled fin-metal foam metal hydride bed towards enhanced hydrogen absorption performance of metal hydride hydrogen storage device. *Energy*. **2022,** *243*, 123044.

[43] Wang, M.; Jiang, C.; Zhang, S. Song, X.; Tang, Y.; Cheng, H. M. Reversible calcium alloying enables a practical room-temperature rechargeable calcium-ion battery with a high discharge voltage. *Nature Chem*. **2018,** *10*, 667-672.

[44] Mu, S.; Liu, Q.; Kidkhunthod, P.; Zhou, X.; Wang, W.; Tang, Y. Molecular grafting towards high-fraction active nanodots implanted in N-doped carbon for sodium dual-ion batteries. *Natl. Sci. Rev*. **2021,** *8*, 178.

[45] Dennington, R.; Keith, T. A.; Millam, J. M. *GaussView*; Shawnee Mission (KS): Semichem Inc., 2016.

[46] Frisch, M. J.; Trucks, G. W.; Schlegel, H. B.; Scuseria, G. E.; Robb, M. A.; Cheeseman, J. R.; Scalmani, G.;

Barone, V.; Petersson, G. A.; Nakatsuji, H.; Li, X.; Caricato, M.; Marenich, A. V.; Bloino, J.; Janesko, B. G.; Gomperts, R.; Mennucci, B.; Hratchian, H. P.; Ortiz, J. V.; Izmaylov, A. F.; Sonnenberg, J. L.; Williams-Young, D.; Ding, F.; Lipparini, F.; Egidi, F.; Goings, J.; Peng, B.; Petrone, A.; Henderson, T.; Ranasinghe, D.; Zakrzewski, V. G.; Gao, J.; Rega, N.; Zheng, G.; Liang, W.; Hada, M.; Ehara, M.; Toyota, K.; Fukuda, R.; Hasegawa, J.; Ishida, M.; Nakajima, T.; Honda, Y.; Kitao, O.; Nakai, H.; Vreven, T.; Throssell, K.; Montgomery, J. A., Jr.; Peralta, J. E.; Ogliaro, F.; Bearpark, M. J.; Heyd, J. J.; Brothers, E. N.; Kudin, K. N.; Staroverov, V. N.; Keith, T. A.; Kobayashi, R.; Normand, J.; Raghavachari, K.; Rendell, A. P.; Burant, J. C.; Iyengar, S. S.; Tomasi, J.; Cossi, M.; Millam, J. M.; Klene, M.; Adamo, C.; Cammi, R.; Ochterski, J. W.; Martin, R. L.; Morokuma, K.; Farkas, O.; Foresman, J. B.; Fox, D. J. *Gaussian 16*; Gaussian, Inc. Wallingford CT, 2016.

[47] Perdew, J. P.; Burke, K.; Ernzerhof, M. Generalized gradient approximation made simple. *Phys. Rev. Lett*. **1996,** *77*, 3865.

[48] Lehtola, S. A review on non-relativistic fully numerical electronic structure calculations on atoms and diatomic molecules. *Int. J. Quantum Chem*. **2019,** *119*, e25968.

[49] Henkelman, G.; Arnaldsson, A.; Jónsson, H. A fast and robust algorithm for Bader decomposition of charge density. *Comput. Mater. Sci*. **2006,** *36*, 354-360.

[50] Zhou, Y. G.; Zu, X. T.; Gao, F.; Xiao, H. Y.; Lv, H. F. Electronic and magnetic properties of graphene absorbed with S atom: A first-principles study. *J. Appl. Phys*. **2009,** *105*, 104311.

[51] Mao, Y.; Yuan, J.; Zhong, J. Density functional calculation of transition metal adatom adsorption on graphene. *J. Phys. Condens. Matter*. **2008,** *20*, 115209.

[52] Young, H. A.; Freedman, R. D. *Sears and Zemansky's University Physics with Modern Physics*. 13th ed.; Boston: Addison-Wesley, 2012; pp 754.

[53] Zeng, K.; Xu, R.; Lu, T.; Tian, Z.; Jiang, P. NMR measurements for gas adsorption characterization on shale: state of the art and perspectives. *Energy Fuels*. **2023,** *37*, 8824-8835.

[54] Witherspoon, V. J.; Xu, J.; Reimer, J. A. Solid-State NMR investigations of carbon dioxide gas in metal-organic frameworks: Insights into molecular motion and adsorptive behavior. *Chem. Rev*. **2018,** *118*, 1003310048.